JOURNAL OF AGRICULTURAL AND FOOD CHEMISTRY

pubs.acs.org/JAFC

Article

Xanthomonas campestris Employs the RND Family Pump HepABCD for Phenolic Acid Efflux and Enhancing Viability and Antioxidant Activity

Kai Song, Ying Cui, Lin Li, Jia-Yuan Wang, Si-Nan Li, Yu-Cheng Gu, Ya-Wen He,* and Lian Zhou*

Cite This: *J. Agric. Food Chem.* 2025, 73, 17458−17470

Read Online

ACCESS | Metrics & More | Article Recommendations | Supporting Information

ABSTRACT: *Xanthomonas campestris* pv. *campestris* (Xcc) is the causal pathogen of black rot in cruciferous plants. Upon infection, Xcc triggers the accumulation of some phenolic acids in the host plants. The mechanism by which Xcc copes with these defense compounds remains unclear. Here, we revealed that Xcc exports benzoic acid, cinnamic acid, and their monohydroxylated derivatives through the resistance-nodulation-division family efflux pump HepABCD. This efflux system influenced glutathione and catalase levels in the wild-type strain XC1, affecting cell viability and modulating ROS levels. We identified HepR as a sensor for 4-hydroxybenzoic acid (4-HBA). The tryptophan residue W22 is critical for HepR binding to 4-HBA. Binding of 4-HBA caused HepR to dissociate from its promoter P_{hep} and induced *hepABCD* expression. Additionally, HepR acts as a redox sensor, and cysteine-to-serine mutations at C39 or C77 significantly reduced its binding affinity to P_{hep}. Collectively, these findings highlight the crucial role of phenolic acid efflux in *Xcc* viability and host colonization.

KEYWORDS: *Xanthomonas campestris pv. campestris, RND family efflux pump, 4-hydroxybenzoic acid, reactive oxygen species, sensor*

INTRODUCTION

Xanthomonas campestris pv. *campestris* (Xcc) is the causal pathogen of black rot disease in crucifers. It is an extensively studied pathogen and is widely used as a model strain for investigating plant−pathogen interaction.[1,2] As a vascular pathogen, Xcc enters plant tissues through leaf margin hydathodes, stomata, and wounds. Xcc infection causes symptoms of vascular tissue blackening and foliar lesions, leading to chlorosis or necrosis in severe cases. Ultimately, this disease results in vegetable rot, rendering the agricultural products unsuitable for consumption.[3]

Phenolic acids are commonly produced and accumulated in the subepidermal layers of plant tissue when plants are exposed to stress and pathogen attack.[4] These phenolic acids possess a wide range of antimicrobial properties and function as defense compounds by disrupting membrane integrity and decoupling the respiratory proton gradient.[5,6] 4-Hydroxybenzoic acid (4-HBA) is recognized as one of the most significant phenolic compounds involved in plant defense against pathogen attacks, with cabbage producing it at micromolar levels.[7] Additionally, its biosynthesis in cell cultures of carrot and potato can be enhanced through treatment with pathogenic fungal elicitors.[8] Meanwhile, some plant pathogens have evolved mechanisms to use these compounds as a carbon source by degrading them through enzymatic pathways.[9,10] Previous studies reported that Xcc degrades 4-hydroxycinnamic acid (4-HCA), ferulic acid, and sinapic acid via HcaLDH.[11] The degradation product of 4-HCA, 4-HBA, is further converted into protocatechuate (PCA) by 4-hydroxybenzoate hydroxylase PobA.[7,11] Subsequently, PCA is metabolized into succinyl-CoA and acetyl-CoA through the *β*-ketoadipate shunt.[12] Both Δ*pobA* and Δ*hcaLDH* mutants exhibited significantly reduced pathogenicity, suggesting that 4-HBA and its analogs pose a stress challenge to Xcc during host plant infection.[7,12]

In addition to degrading phenolic compounds, plant pathogens may have evolved the ability to exploit plant signals to activate efflux pumps. This enables pathogens to expel antimicrobial substances and ensure bacterial survival in hostile host environments.[13,14] In *Dickeya dadantii*, the efflux pump genes *acrAB* and *emrAB* were shown to be associated with virulence and induced by the plant defense signal salicylic acid (SA) together with its precursors.[15] Additionally, mutation of *tolC*, an outer membrane-encoding gene *tolC*, confers *D. dadantii* hypersensitivity to plant-derived phenolic acids, including *p*-coumaric acid and *t*-cinnamic acid.[16] Although Xcc is known to degrade certain phenolic acid compounds, there are phenolic acids in plants that Xcc cannot degrade. It is known that the resistance-nodulation-division (RND) efflux pump HepABCD of Xcc is also activated by SA, enhancing Xcc virulence in host plants.[17] These clues prompted us to investigate whether HepABCD is involved in the efflux of *Xcc*-associated phenolic compounds.

In this study, we identified that HepABCD mediated the efflux of 4-HBA, benzoic acid, cinnamic acid, and their monohydroxylated derivatives. Additionally, HepABCD was found to be crucial for enhancing antioxidant activity and maintaining Xcc

Received: March 24, 2025
Revised: June 20, 2025
Accepted: June 25, 2025
Published: July 4, 2025

viability. This study also explored the regulatory mechanism of HepR as a dual sensor for both 4-HBA and redox status. Our findings indicated that HepR regulated *hepABCD* expression by binding to 4-HBA and sensing redox changes, thereby facilitating phenolic acid efflux and enhancing Xcc virulence and survival within host plants.

MATERIALS AND METHODS

Bacterial Strains and Growth Conditions. The bacterial strains and plasmids used in this study are given in Tables S1 and S2. The wild-type strain XC1 and its derivatives were cultured at 28 °C in XYS medium (0.7 g/L K_2HPO_4, 0.2 g/L KH_2PO_4, 1 g/L $(NH_4)_2SO_4$, 0.1 g/L $MgCl_2{\cdot}6H_2O$, 0.01 g/L $FeSO_4{\cdot}7H_2O$, 0.001 g/L $MnCl_2{\cdot}4H_2O$, 5 g/L sucrose, 0.0625% yeast extract, pH 7.0) or NYG medium (5 g/L peptone, 3 g/L yeast extract, 20 g/L glycerol). Tryptone, peptone, beef extract, and yeast extract were procured from Sangon Biotech (Shanghai, China). *E. coli* DH5α was used as the host for constructing all recombinant vectors. *E. coli* strains were cultured at 37 °C in LB medium (5 g/L yeast extract, 10 g/L peptone, 10 g/L sodium chloride). When required, antibiotics were added at the following concentrations: rifamycin (Rif), 25 μg/mL; kanamycin (Km), 50 μg/mL; ampicillin (Amp), 100 μg/mL. Bacterial growth was monitored by measuring the optical density at a wavelength of 600 nm.

Gene Deletion and Complementation. Xcc deletion mutants were constructed using the *sacB*-mediated double homologous recombination method. Briefly, the upstream and downstream fragments of the target gene were initially amplified via PCR using the primers listed in Table S3. The fragments were then cloned into the pK18mobsacB vector to generate a recombinant plasmid using a ClonExpress MultiS one-step cloning kit (Vazyme, China). The recombinant plasmid was subsequently transformed into *E. coli* S17-1λpir and transferred into Xcc through a biparental mating process. Subsequently, colonies exhibiting resistance to both Km and Rif and sensitivity to sucrose were selected on NRK (NYG supplemented with Km and Rif) and NAS media (NA containing 5% sucrose), respectively. The target gene deletion was confirmed by PCR and sequencing analysis using the primers listed in Table S3.

Assay for Xcc Tolerance to 4-HBA and Its Analogs. To initially assess the tolerance of Xcc to 4-HBA and its structural analogs, single colonies were inoculated into NYG medium supplemented with Rif and incubated at 28 °C for 12 h. The bacterial cultures were then harvested by centrifugation at 11,200*g* for 5 min and washed twice with 1× PBS. The resulting bacterial pellets were resuspended in 1 mL of 1× PBS. The suspensions were serially diluted and spotted onto XYS agar plates, with or without 1 μM or 3 mM 4-HBA and various structural analogs of 4-HBA. The tolerance to each compound was assessed by evaluating bacterial growth.

Extraction and Quantitative Analyses of 4-HBA in XC1 Cultures. 4-HBA was extracted and purified from XC1 cultures in accordance with the methods previously described.[18] The levels of 4-HBA production were subsequently quantified using high-performance liquid chromatography (HPLC), as described in the same study. Briefly, 0.5 mL of culture supernatant of the XC1 strain and its derived variants were adjusted to a pH of 3.5 and extracted with 1 mL of ethyl acetate. The ethyl acetate fractions were collected, evaporated, and reconstituted in 0.1 mL of methanol for HPLC analysis with a C18 reversed-phase column (Zorbax XDB; 5 μm, 4.6 × 150 mm). The mobile phase comprised methanol and water, each containing 0.05% formic acid, in a ratio of 25/75 (v/v), with a flow rate of 1 mL min^{-1}. Commercially available 4-HBA (Sigma, USA) was used as the standard for calibration.

Intracellular 4-HBA in Xcc Extraction and Measurement. To extract the intracellular 4-HBA of Xcc, 50 mL of each culture was collected 12 hpi and centrifuged at 10,000*g* for 30 min at 4 °C, and the bacterial cell pellets were washed three times with 1× PBS. Subsequently, the bacteria were resuspended in 10 mL of B-PER bacterial protein extraction reagent and incubated at room temperature for 30 min to completely lyse the cells. Following this, the lysate was centrifuged at 11,200*g* for 10 min, and the supernatant was collected for 4-HBA extraction following the method described.[7] Briefly, 10 mL of the supernatant was adjusted to a pH of 4.0 and extracted with 20 mL of ethyl acetate. The ethyl acetate layer was then separated and evaporated by using a rotary evaporator. Finally, the remaining residues were dissolved in 0.1 mL of methanol for further analysis.

For the quantitative analysis of intracellular 4-HBA levels, HPLC combined with triple quadrupole tandem mass spectrometry (HPLC-QqQ-MS/MS) was employed (Agilent, California, USA). Briefly, 10 μL of the extract was loaded onto a Zorbax Eclipse XDB-C18 column (Agilent, 4.6 × 150 mm, 5 μm) for chromatographic separation. The column was eluted with a mixture of methanol containing 0.1% formic acid and water at a flow rate of 0.4 mL/min over 40 min, and the volume ratio was set to 40/60. Quantitative analysis was conducted using a QqQ-MS/MS with an electrospray ionization ion source (Agilent, California, USA). The mass spectrometry spectra were recorded in multiple-reaction monitoring mode. The cytoplasmic 4-HBA level was expressed as the concentration of 4-HBA per 1×10^9 bacterial cells.

Protein Expression and Purification. HepR protein was purified in accordance with previously established protocols.[17] In brief, a single colony of BL21(DE3) harboring the recombinant vector pET28a-HepR was inoculated into LB medium supplemented with kanamycin and incubated for 8 h at 37 °C. The initial culture was transferred to 500 mL of liquid LB containing Km and grown at 37 °C until an optical density (OD_{600}) of 0.6 was attained. The bacteria were then induced with 0.1 mM isopropyl-β-D-thiogalactopyranoside and further cultivated for an additional 16 h at 16 °C.

Following induction, the bacterial cells were harvested by centrifugation at 4 °C and 4000*g* for 10 min and then washed twice with 1× PBS. The cells were resuspended in HEPES buffer A (25 mM HEPES, 150 mM NaCl, 10 mM imidazole, pH 7.4), disrupted by sonication, and centrifuged at 13,800*g* and 4 °C for 40 min. The supernatant was collected and loaded onto a Ni-NTA column (Smart-Lifesciences, Shanghai, China). The proteins were eluted from the column using 250 mM imidazole in HEPES buffer. The eluted fractions were pooled and analyzed via sodium dodecyl sulfate-polyacrylamide gel electrophoresis (SDS-PAGE). The fraction containing His-tagged HepR was concentrated and subjected to size exclusion chromatography using a Superdex 75 gel filtration column (GE Healthcare), which was equilibrated with a buffer without imidazole (25 mM HEPES and 150 mM NaCl, pH 7.4).

Isothermal Titration Calorimetry Assay. The binding affinity between 4-HBA and HepR was measured using ITC following the manufacturers' protocols. Both the HepR protein and 4-HBA were prepared in HEPES buffer (25 mM HEPES, 150 mM NaCl, pH 7.4) prior to titration. All solutions were centrifuged at 11,200*g* for 10 min before use. For each ITC measurement, 400 μL of HepR protein was injected into a cuvette. Any excess was aspirated using a syringe. The 4-HBA molecule was then aspirated with a buret, ensuring that it was free of air bubbles. The titration was conducted at 18 °C with a stirring speed of 750 rpm. The binding capacity between HepR and 4-HBA was measured using a MicroCal ITC200 isothermal titration calorimeter (GE Healthcare, Chicago, USA).

Surface Plasmon Resonance (SPR) Assay. The interaction between HepR and 4-HBA was analyzed by SPR assay using a Biacore 8K instrument (Cytiva, Sweden). The assay was performed in phosphate-buffered saline (PBS) supplemented with 0.25% Tween at 25 °C. His-tagged HepR was immobilized onto a CM5 Sensor Chip via a standard amine-coupling procedure in 10 mM sodium acetate (pH 5.0). Serial dilutions of 4-HBA were injected onto the sensor chip at a flow rate of 30 μL/min for 120 s, followed by a 120 s buffer flow. The dissociation constant (K_d) was determined by using the accompanying evaluation software.

Electrophoretic Mobility Shift Assay (EMSA). EMSA was conducted in accordance with an established protocol.[7] In brief, various concentrations of 4-HBA and purified His-HepR were combined with a Cy5-labeled promoter fragment, P_{hep}, in 20 μL of EMSA buffer consisting of 20 mM Tris (pH 7.9), 10 mM $MgCl_2$, 5% glycerol, 40 μg of BSA, and 100 ng of denatured salmon sperm DNA. The resulting mixtures were then applied to a 4.5% native polyacrylamide gel and subjected to electrophoresis in 0.5× TB buffer for 90 min. Following electrophoresis, the Cy5 fluorophore within the

https://doi.org/10.1021/acs.jafc.5c03670
J. Agric. Food Chem. 2025, 73, 17458−17470

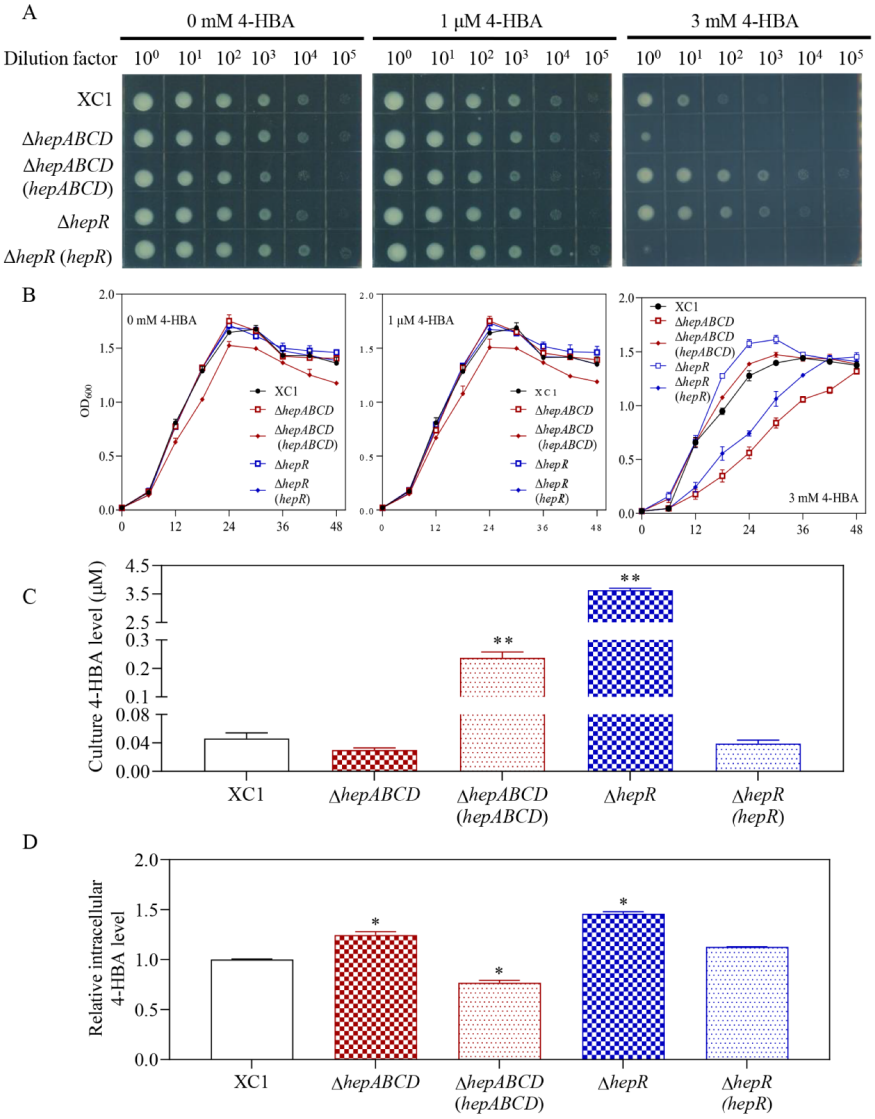

Figure 1. HepABCD is responsible for 4-HBA efflux. (A) Growth of XC1, Δ*hepABCD*, Δ*hepABCD* (*hepABCD*), Δ*hepR*, and Δ*hepR* (*hepR*) on XYS agar plates with or without 1 μM or 3 mM 4-HBA. (B) Growth of XC1, Δ*hepABCD*, Δ*hepABCD* (*hepABCD*), Δ*hepR*, and Δ*hepR* (*hepR*) in XYS liquid medium with or without 1 μM or 3 mM 4-HBA. (C) Extracellular 4-HBA levels of the Xcc strains XC1, Δ*hepABCD*, Δ*hepABCD* (*hepABCD*), Δ*hepR*, and Δ*hepR* (*hepR*) in XYS medium 12 hpi. (D) Intracellular 4-HBA levels of the Xcc strains XC1, Δ*hepABCD*, Δ*hepABCD* (*hepABCD*), Δ*hepR*, and Δ*hepR* (*hepR*) 12 hpi. Shown are the averages of three technical repeats with the standard deviation. Statistically significant differences are indicated by one asterisk ($p < 0.05$) or two asterisks ($p < 0.01$).

gel was detected by utilizing an Amersham Typhoon RGB biomolecular imager (Cytiva, Sweden).

***β*-Glucuronidase (GUS) Activity Assay.** The *gusA*-based reporter strain construction and the quantitative GUS activity assays were conducted in accordance with previously established methods.[11] In brief, the reporter strains were cultivated in XYS medium at a constant temperature of 28 °C. Following cultivation, bacterial cells were harvested and subjected to centrifugation at 13,800*g* for 10 min and then washed once with 1× PBS. The bacterial cells were resuspended in 1 mL of PBS buffer and disrupted with 20 μL of a 0.1% (w/v) SDS solution and 40 μL of chloroform. GUS activity was quantified by assessing fluorescence intensity using 4-methylumbelliferone-D-glucuronide as the substrate with an excitation wavelength of 365 nm and an emission wavelength of 455 nm.

Bacterial Viability Assay. To visualize bacterial activity, single colonies were inoculated into NYG medium supplemented with Rif and incubated at 28 °C for 12 h. Each culture was then transferred into 50 mL of liquid XYS and incubated at 28 °C and 200 rpm. At 24 and 48 hpi, 1 mL of bacterial culture was collected by centrifugation at 11,200*g* for 10 min and washed twice with 1× PBS. The bacterial pellet was resuspended in 1 mL of 1× PBS. The resuspended cells were serially diluted, and 2 μL of each dilution was spotted onto XYS plates to assess bacterial viability during cultivation.

ROS Measurements. ROS levels in XC1 were measured as previously described. At 24 and 48 hpi, 1 mL of each culture was centrifuged at 11,200*g* for 10 min. The bacterial pellets were then treated with 1 mL of 10 μM 2′,7′-dichlorodihydrofluorescein diacetate and incubated at 28 °C for 30 min. Following incubation, the cells were washed twice with 1× PBS. The fluorescence intensity was measured using a microplate reader with excitation at 488 nm and emission at 525 nm.

GSH Determination. GSH concentrations were determined by using a GSH assay kit (Beyotime, China). Briefly, 1 mL of bacterial culture was centrifuged at 12,000*g* for 10 min to harvest the cells. The resulting cell pellets were subsequently washed twice with 1× PBS. Then, 30 μL of reagent M solution (provided in the commercial assay kit) was added to remove protein, and the mixture was placed in liquid nitrogen and then in a 37 °C water bath two or three times. The samples were placed on ice or stored at 4 °C for 5 min. Subsequently, the mixture was centrifuged at 10,000*g* for 10 min at 4 °C to remove cell

https://doi.org/10.1021/acs.jafc.5c03670
J. Agric. Food Chem. 2025, 73, 17458−17470

debris and proteins, and the supernatant was collected to quantify GSH levels using a preprepared standard curve.

Catalase Activity Assay. To measure catalase activity, 0.5 mL of bacterial culture was centrifuged at 12,000*g* for 10 min to harvest the cells, and the bacterial cell pellets were washed three times with 1× PBS. Subsequently, the bacteria were suspended in 1 mL of B-PER® bacterial protein extraction reagent and reacted for 30 min at room temperature to fully lyse the cells, followed by centrifugation at 12,000*g* for 10 min. The protein concentration was measured using a Bradford dye reagent (Takara, Japan). The supernatant was used to measure catalase activity using a catalase assay kit (Beyotime, China) according to the manufacturer's instructions. One unit represented the amount of enzyme that catalyzed the decomposition of 1 μM H_2O_2 per minute at 25 °C. A calibration curve was plotted by using a defined unit of catalase activity.

Bioinformatics Analysis. All DNA sequences, amino acid sequences, and genome sequences were obtained from the NCBI database (https://www.ncbi.nlm.nih.gov/). Protein domain organization was predicted using the SMART program (https://smart.embl.de/smart/set_mode.cgi?NORMAL=1). Promoter prediction was performed using the Prokaryote Promoter Prediction tool (http://genome2d.molgenrug.nl/g2d_pepper_promoters.php). Multiple sequence alignment analysis was performed using Clustal Omega (https://www.ebi.ac.uk/Tools/msa/clustalo/).

Statistical Analyses. All experiments were performed independently at least three times. Data are presented as means ± standard deviation (SD). For comparisons between two groups, unpaired *t*-tests were used. For comparisons among multiple groups, one-way or two-way analysis of variance (ANOVA) was performed, followed by the least significant difference (LSD) test, as appropriate. Statistical significance was indicated as follows: ns, no significance; *, $p < 0.05$; **, $p < 0.01$.

RESULTS

HepABCD Is Responsible for 4-HBA Efflux. 4-HBA, a phenolic compound abundantly produced by plants, was shown to have a markedly increased concentration during pathogen infections, highlighting its role in plant defense mechanisms.[19] In addition to its defensive role, 4-HBA regulates various bacterial biological processes.[18,20] A previous study demonstrated that the AaeXAB efflux pump in *Escherichia coli* mediated the efflux of 4-HBA.[21] To identify homologous sequences in Xcc, a BlastP search was conducted using the AaeXAB amino acid sequences as a query against the genome of Xcc strain ATCC33913. The homologous protein HepB (Xcc4169) was shown to share a 40.55% amino acid identity and a similar domain configuration with AaeA. Although AaeX and AaeB exhibited lower similarity to HepA (Xcc4168) and HepD (Xcc4171), their domains, as predicted by the SMART program, were similar (Figure S1).

The *hepR* and *hepABCD* (*Xcc4167-4171*) genes were previously shown to be cotranscribed within a single gene cluster. Among these, *hepABCD* encodes an RND efflux pump, known as the SA efflux pump, while *hepR* encodes a negative regulator that binds to an AT-rich region in the promoter of the *hepR-hepABCD* gene cluster.[17] To evaluate whether the HepABCD pump protects *Xcc* against elevated 4-HBA levels, a deletion mutant Δ*hepABCD* and a *hepABCD* complementation strain Δ*hepABCD* (*hepABCD*) were constructed. The strains were cultured in NYG broth for 12 h, then serially diluted and spotted onto XYS agar, with or without 1 μM or 3 mM 4-HBA, to assess their growth. In the absence of 4-HBA, no differences in growth were observed on XYS agar plates among the wild-type XC1, Δ*hepABCD*, or Δ*hepABCD* (*hepABCD*) strains (Figure 1A). Similarly, 1 μM 4-HBA had no significant effect on the growth of any Xcc strain (Figure 1A). Since Xcc degrades 4-HBA during growth, a higher concentration of 3 mM 4-HBA was used to investigate its inhibitory effect. In the presence of 3 mM 4-HBA, strain Δ*hepABCD* failed to grow, while strains XC1 and Δ*hepABCD* (*hepABCD*) exhibited certain tolerance (Figure 1A). Interestingly, the Δ*hepR* mutant, which overexpressed the *hepABCD* genes,[17] showed moderately enhanced resistance to 3 mM 4-HBA compared to XC1. Additionally, overexpression of *hepR* with the pBBRMCS-2 vector in the Δ*hepR* strain significantly reduced the tolerance to 4-HBA (Figure 1A). Interestingly, the growth rate of the Δ*hepABCD* mutant in XYS liquid medium supplemented with 4-HBA was lower than that of the wild-type strain, although its final population was only partially limited (Figure 1B). Under the same conditions, the complementation strain Δ*hepABCD* (*hepABCD*) showed improved growth (Figure 1B), as expected. The Δ*hepR* mutant also exhibited better growth in XYS liquid medium supplemented with 3 mM 4-HBA compared to XC1, whereas the complementation strain Δ*hepR* (*hepR*) grew poorly (Figure 1B).

To confirm the role of HepABCD in 4-HBA efflux, extracellular and intracellular 4-HBA levels of wild-type and mutant strains cultured in XYS medium were measured 12 h post-inoculation (hpi). The extracellular 4-HBA concentrations of XC1, Δ*hepABCD*, and Δ*hepABCD* (*hepABCD*) were 0.05, 0.03, and 0.24 μM, respectively (Figure 1C), while the relative intracellular 4-HBA levels in strains Δ*hepABCD* and Δ*hepABCD* (*hepABCD*) were approximately 124% and 77% of those observed in XC1, respectively, (Figure 1D). The Δ*hepR* strain's extracellular 4-HBA concentrations reached 3.63 μM, 78.5 times higher than that of the wild-type strain. In contrast, the *hepR* complementation strain had an extracellular 4-HBA concentration restored to 0.04 μM, a level comparable to that of wild-type strain XC1 (Figure 1C). These findings demonstrated that HepABCD mediated 4-HBA efflux.

HepABCD Mediates Efflux of Benzoic Acid, Cinnamic Acid, and Their Monohydroxylated Derivatives. The AaeXAB efflux pump was previously reported to mediate the efflux of multiple compounds, namely 4-HBA, 6-hydroxy-2-naphthoic acid, and 2-hydroxycinnamate.[21] To identify other substrates of the HepABCD efflux pump, we assessed the tolerance of strains XC1, Δ*hepABCD*, and Δ*hepABCD* (*hepABCD*) to a range of compounds, including benzoic acid (BA), hydroxybenzoic acids (HBAs), cinnamic acid (CA), hydroxycinnamic acids (HCAs), and other 4-HBA structural analogs (Table 1). The Δ*hepABCD* (*hepABCD*) strain exhibited similar or higher levels of tolerance to BA, SA, 3-hydroxybenzoic acid (3-HBA), CA, 2-hydroxycinnamic acid (2-HCA), 3-hydroxycinnamic acid (3-HCA), 4-hydroxycinnamic acid (4-HCA), vanillic acid, and ferulic acid than XC1 (Figure 2, Table 1). In contrast, strain Δ*hepABCD* displayed significantly reduced tolerance to these compounds (Figure 2). Additionally, all of the examined strains displayed comparable growth rates on XYS agar plates supplemented with BA or CA derivatives containing multiple hydroxyl groups (Figure S2, Table 1). These results suggested that the HepABCD efflux pump exhibited a high degree of specificity for benzoic acid and cinnamic acid and their monohydroxylated derivatives.

HepABCD Efflux Pump Influences Bacterial Reactive Oxygen Species (ROS) Levels and Xcc Viability. The AaeAB efflux system is thought to be a regulatory mechanism that primarily responds to intracellular stress conditions.[21] To evaluate the effect of *hepR-hepABCD* on Xcc viability, strains XC1, Δ*hepR*, Δ*hepABCD*, and their respective complementa-

https://doi.org/10.1021/acs.jafc.5c03670
J. Agric. Food Chem. 2025, 73, 17458−17470

Table 1. Efflux Capacity of *hepABCD* for 4-HBA Structural Analogs

Classification	Compound	Efflux capacity
Benzoic acid and hydroxybenzoic acid	Benzoic acid	√
	2-hydroxybenzoic acid	√
	3-hydroxybenzoic acid	√
	4-hydroxybenzoic acid	√
	2,3-Dihydroxybenzoic acid	×
	2,4-Dihydroxybenzoic acid	×
	2,5-Dihydroxybenzoic acid	×
	2,6-Dihydroxybenzoic acid	×
	3,4-Dihydroxybenzoic acid	×
	3,5-Dihydroxybenzoic acid	×
	Gallic acid	×
	Vanillic acid	√
Cinnamic acid and hydroxycinnamic acid	Cinnamic acid	√
	2-hydroxycinnamic acid	√
	3-hydroxycinnamic acid	√
	4-hydroxyinnamic acid	√
	Caffeic acid	×
	Ferulic Acid	√
Other structural analogs	Salicin	×
	Coumarin	×
	DL-2-Piperidinecarboxylic acid	×
	Vanillin	×

tion strains were cultured in XYS medium. The cells were collected at 24 and 48 hpi, and their suspension was serially diluted and spotted onto XYS agar plates. No significant differences in the number of colony-forming units (CFUs) were observed among the strains collected at 24 hpi (Figure 3A). At 48 hpi, the cultures reached the late stationary phase and exhibited similar optical densities (Figure 1B). However, although the Δ*hepABCD* deletion mutant showed a significant reduction in the level of CFUs, its complementation strain Δ*hepABCD* (*hepABCD*) demonstrated a notable increase in viability (Figure 3A). Similarly, the Δ*hepR* mutant with overexpression of *hepABCD* showed enhanced viability compared with the wild-type XC1 strain. Conversely, overexpression of *hepR* in the Δ*hepR* mutant strain [Δ*hepR* (*hepR*)] led to significantly reduced CFUs on XYS agar (Figure 3A). Quantitatively, the CFU counts of strains XC1, Δ*hepABCD*, Δ*hepABCD* (*hepABCD*), Δ*hepR*, and Δ*hepR* (*hepR*) at 48 hpi were 2.70×10^6, 2.57×10^4, 1.64×10^9, 1.39×10^8, and 1.30×10^4 CFU/mL, respectively, (Figure 3B). These results underscore the regulatory role of the *hepR-hepABCD* module, which maintains bacterial viability during the late growth phase.

ROS can damage various macromolecules, including DNA, RNA, proteins, and lipids, ultimately compromising cell viability.[22] To further explore how the *hepR-hepABCD* cluster influenced bacterial viability, ROS levels were assessed in Δ*hepR* and Δ*hepABCD* after culturing for 24 and 48 h. At 24 hpi, there were no significant differences in the ROS levels among the tested strains (Figure 3C). At 48 hpi, both the Δ*hepR* and Δ*hepABCD* (*hepABCD*) strains showed significantly reduced ROS levels compared to XC1, whereas strains Δ*hepR* (*hepR*) and Δ*hepABCD* had significantly higher levels (Figure 3C). These results suggested a potential role of the HepABCD efflux pump in regulating ROS levels, particularly at a later stage of bacterial growth.

The HepABCD Efflux Pump Is Involved in Modulating the Levels of Catalase and GSH in Xcc. Bacteria use both enzymatic and nonenzymatic ROS scavengers to protect against oxidative stress caused by ROS.[23,24] For example, catalase counteracts ROS by catalyzing the decomposition of H_2O_2,[25] while glutathione (GSH), a major antioxidant, reduces cellular damage by tightly regulating ROS levels.[26,27] To explore the role of the HepABCD efflux pump in modulating ROS levels, we evaluated the GSH levels and catalase activity in the mutant strains. At 24 hpi, no significant differences were observed in the GSH levels or catalase activity among the five tested strains. However, by 48 hpi, the strain with *hepABCD* deleted had reduced GSH levels and catalase activity, while the strain with *hepABCD* overexpressed showed increased GSH levels and catalase activity. Conversely, XC1 with *hepR* deleted exhibited significantly increased GSH levels and catalase activity compared to strain XC1, whereas strain Δ*hepR* with *hepR* overexpression exhibited levels lower than those of XC1 (Figure 4). These results indicate that HepR negatively regulates catalase activity and GSH levels via HepABCD, thereby contributing to the antioxidant defense and viability of *Xcc*.

HepR Is a 4-HBA Sensor. A recent study identified HepR as an SA sensor, whose binding to SA triggers the dissociation of HepR from the *hep* promoter and induces the expression of the *hep* gene cluster.[17] We further investigated whether HepR also functioned as a sensor for 4-HBA. Previous studies demonstrated that Xcc synthesized 4-HBA through the action of XanB2 and subsequently degraded it via PobA (Figure 5A).[18] Accordingly, deleting *xanB2* should decrease intracellular levels of 4-HBA, whereas deleting *pobA* should increase intracellular accumulation. We generated Δ*xanB2* and Δ*pobA* strains with a chromosomally integrated promoter-*gusA* fusion reporter to monitor the putative promoter activity of the 531-bp region upstream of *hepR*. The expression level of the *hep* gene cluster was measured by *β*-glucuronidase (GUS) activity. Our results showed that expression of the *hep* gene cluster was higher in the Δ*pobA*::P_{hep}-*gusA* strain and lower in the Δ*xanB2*::P_{hep}-*gusA* strain compared to the XC1:P_{hep}-*gusA* strain (Figure 5B). These findings suggested that fluctuations in the physiological level of 4-HBA influenced *hep* gene cluster expression. Furthermore, treatment with 100 *μ*M 4-HBA upregulated *hep* gene cluster expression in both Δ*pobA*::P_{hep}-*gusA* and Δ*xanB2*::P_{hep}-*gusA* strains (Figure 5B). Together, these results suggested that 4-HBA positively regulated *hep* gene cluster expression.

Previous *in vitro* studies indicated that HepR regulated the expression of the efflux pump-encoding *hepABCD* genes in response to SA at micromolar levels.[17] To investigate whether HepR also senses 4-HBA, isothermal titration calorimetry (ITC) experiments and surface plasmon resonance (SPR) assays were conducted to evaluate the interaction between HepR and 4-HBA. HepR, a 147-amino-acid protein with a calculated molecular weight of 15.8 kDa, was purified to homogeneity using affinity chromatography. Both ITC and SPR experiments revealed that HepR bound to 4-HBA with a dissociation constant (K_d) of 116 ± 13.6 *μ*M (Figure 5C) and 106 ± 11.2 *μ*M (Figure 5D). Electrophoretic mobility shift assays (EMSA) demonstrated that high levels of 4-HBA prevented HepR from binding to the promoter region of the

https://doi.org/10.1021/acs.jafc.5c03670
J. Agric. Food Chem. 2025, 73, 17458−17470

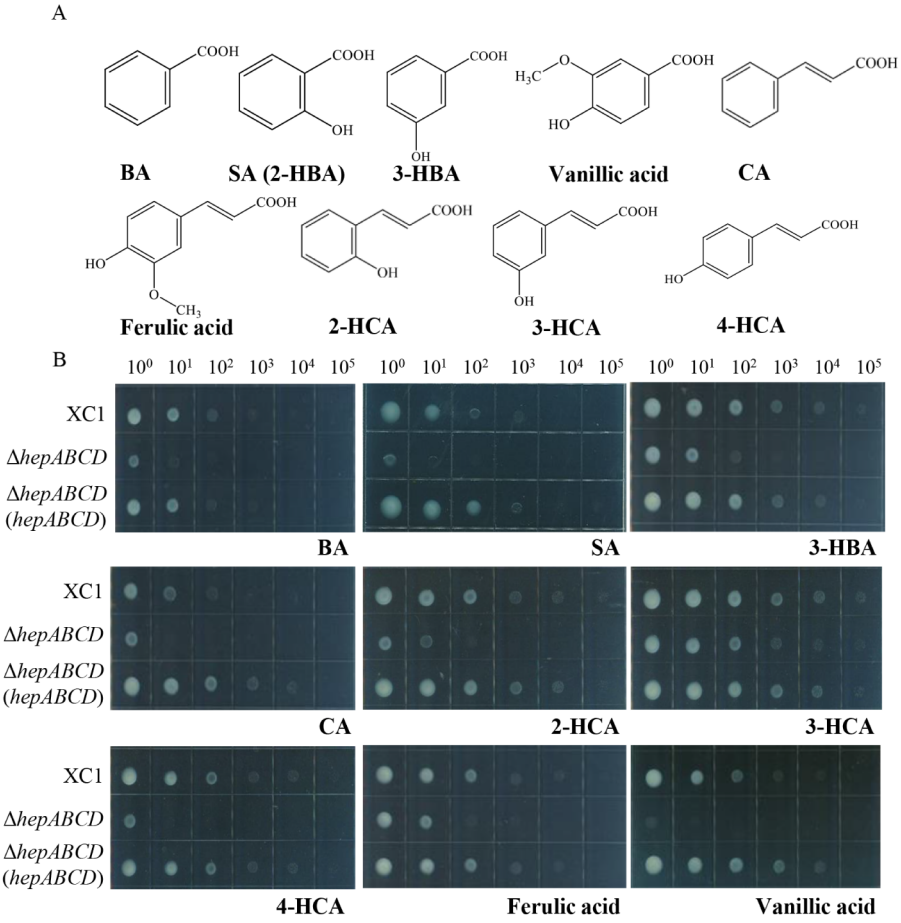

Figure 2. HepABCD mediates the efflux of benzoic acid, cinnamic acid, and their derivatives containing a single hydroxyl group. (A) The chemical structures of 4-HBA analogs used in this study. (B) Growth of XC1, Δ*hepABCD*, and Δ*hepABCD* (*hepABCD*) on XYS agar plates supplemented with 3 mM of each compound. BA: benzoic acid; SA (2-HBA): 2-hydroxybenzoic acid; 3-HBA: 3-hydroxybenzoic acid; CA: cinnamic acid; 2-HCA: 2-hydroxycinnamic acid; 3-HCA: 3-hydroxycinnamic acid; 4-HCA: 4-hydroxycinnamic acid.

hep gene cluster (Figure 5E). Moreover, the exogenous addition of 100 μM 4-HBA did not alter the expression levels of the *hep* gene cluster in the Δ*hepR* strain (Figure 5F). These results indicated that HepR functions as a 4-HBA sensor in Xcc by regulating the expression of the HepABCD efflux pump.

Since the HepR protein of Xcc can sense 4-HBA, SA, and HCAs, it was important to identify the key amino acid residues involved in its binding to these compounds. AlphaFold 3 was used to predict the structure of HepR, and AutoDock was employed to model its interactions with both 4-HBA and SA. The results identified W22 as the shared residue mediating binding to both compounds (Figure S3A). A point mutation substituting tryptophan with alanine (W22A) significantly reduced HepR's binding affinity for both 4-HBA (Figure S3B) and SA (Figure S3C).

A previous study demonstrated that SA significantly induced expression of the *hep* gene cluster in Xcc.[17] Similarly, 100 μM 4-HBA treatment also enhanced the *hep* gene cluster expression in the wild-type strain (Figure 7A). Given that the substrates of HepABCD (4-HBA, SA, CA, 2-HCA) are secondary metabolites produced by plants, we investigated if there are cumulative effects. The expression levels of the *hep* gene cluster were upregulated more markedly by SA, CA, or 2-HCA supplementation in combination with 4-HBA supplementation (Figure S4). These results indicated that 4-HBA analogs can induce a cumulative increase in the expression of the *hep* gene cluster.

HepR Is Also a Redox Sensor. HepR was previously identified as a transcriptional regulator within the MarR family.[17] Because several MarR family regulators are known to function as redox sensors, serving as crucial modulators of bacterial stress responses and virulence,[28−30] the redox-dependent activity of HepR was investigated through *in vitro* EMSA experiments. Adding 50−200 μM DTT to the reaction system enhanced HepR binding to P_{hep} (Figure 6A). However, when 500 μM H_2O_2 was also added to the reaction mixture, HepR was no longer bound to P_{hep}. These observations suggested that the binding affinity between HepR and P_{hep} was modulated by the redox state. Furthermore, adding 50−200 μM 4-HBA and 200 μM DTT to the reaction mixture counteracted the DTT-induced enhancement of HepR binding to P_{hep} (Figure 6A). This result further confirmed the inhibitory effect of 4-HBA on the binding between HepR and P_{hep}.

In bacteria, cysteine thiol groups in proteins often act as thiol-based redox-sensing switches, activating specific detoxification pathways to restore the redox balance.[31] C^{39} and C^{77} are the only two cysteine residues present in HepR. Point mutations of either residue to serine (C39S or C77S) significantly reduced its ability to bind to P_{hep} (Figure 6B). To further investigate whether HepR responds to oxidative stress through cysteine-based redox regulation, strains harboring $HepR^{C39S}$ and $HepR^{C77S}$ mutations were constructed. The extracellular 4-HBA levels of the mutant strains were 0.41 and 0.11 μM, respectively, significantly higher

https://doi.org/10.1021/acs.jafc.5c03670
J. Agric. Food Chem. 2025, 73, 17458−17470

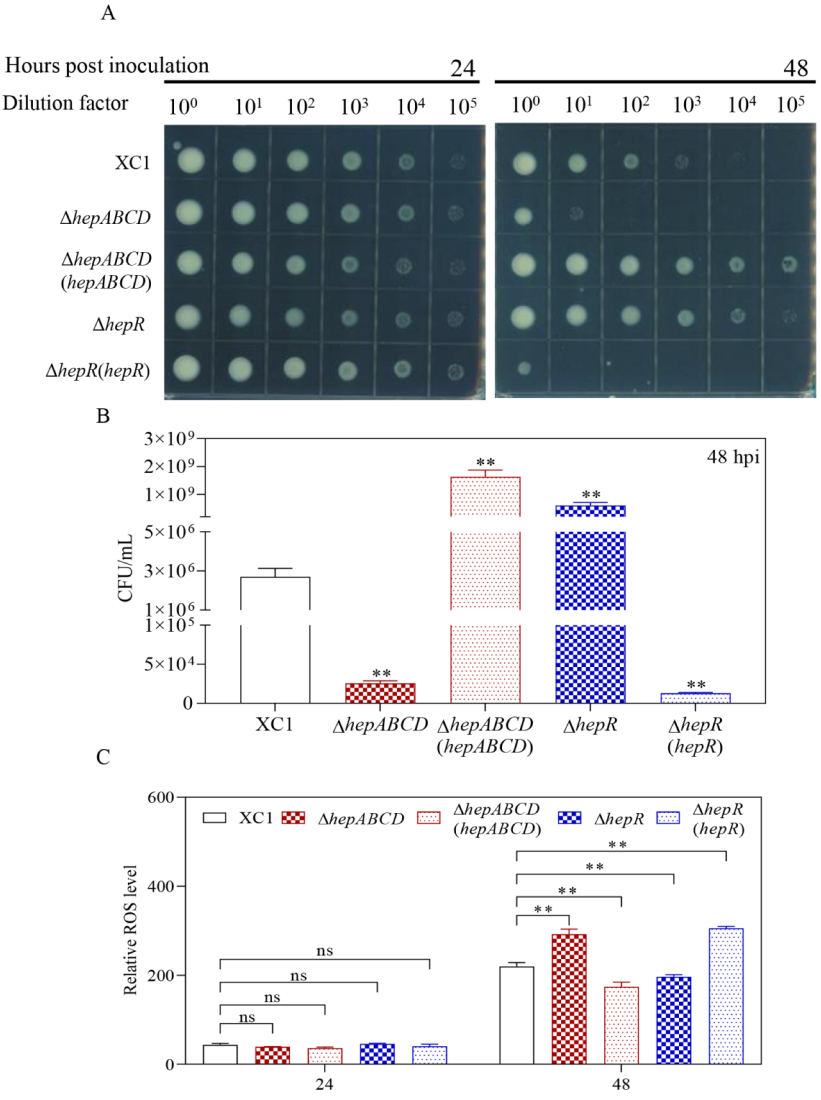

Figure 3. The HepABCD efflux pump influences bacterial reactive oxygen species (ROS) levels and Xcc viability. (A) CFU assays of XC1, Δ*hepABCD*, Δ*hepABCD* (*hepABCD*), Δ*hepR*, and Δ*hepR* (*hepR*) grown in XYS liquid medium at 24 and 48 hpi. (B) Quantitative analysis of the CFUs of XC1, Δ*hepABCD*, Δ*hepABCD* (*hepABCD*), Δ*hepR*, and Δ*hepR* (*hepR*) grown in XYS liquid medium at 48 hpi. (C) Relative ROS levels of XC1, Δ*hepABCD*, Δ*hepABCD* (*hepABCD*), Δ*hepR*, and Δ*hepR* (*hepR*) at 24 and 48 hpi. Shown are the averages of three technical repeats with the standard deviation. Statistically significant differences are indicated by one asterisk ($p < 0.05$) or two asterisks ($p < 0.01$).

than that of the wild-type (0.05 μM) (Figure 6C). Additionally, the cysteine residues C39 and C77 were shown to be critical for HepR and 4-HBA interaction. Supplementing 100 μM 4-HBA did not affect hep gene cluster expression in the C39S and C77S mutants (Figure 7A). Furthermore, ITC experiments showed that the HepR^{C39S} mutant protein failed to interact with 4-HBA (Figure 7B). Taken together, these results demonstrate that HepR acts as a redox sensor to regulate 4-HBA efflux through cysteine residue oxidation.

Distribution of *hepR-hepABCD*/*aaeR-aaeXAB*/*slyA-ydhIJK* Gene Clusters Across Various Bacterial Species. Previous research showed that SlyA acts as an SA-binding protein to regulate the expression of the gene cluster encoding the efflux pump YdhIJK.[32] AaeR functions as a 4-HBA-binding protein that modulates the expression of the AaeXAB efflux system.[21] In this study, HepR was identified as a dual sensor for both SA and 4-HBA, and it can regulate the expression of the *hepR-hepABCD* cluster. To examine the distribution of these systems across bacterial species, homologs of the HepR-HepABCD, AaeR-AaeXAB, and SlyA-YdhIJK systems were identified using BlastP. The results revealed that all three efflux systems are highly conserved in various bacteria. The *hepR-hepABCD* gene cluster was found in *Stenotrophomonas maltophilia* K279a, *Stenotrophomonas pavanii* Y, *Pseudomonas syringae* pv. *syringae* B728a, *Pseudomonas syringae* pv. *tomato* DC3000, *Pseudomonas savastanoi* pv. *savastanoi* NCPPB 3335, *Pseudomonas putida* KT2440, *Acidovorax avenae* subsp. *avenae* ATCC19860, *Acidovorax cattleyae* DSM 17101, *Burkholderia gladioli* BSR3, *Burkholderia glumae* BGR1, *Agrobacterium vitis* VAR03, and *Agrobacterium tumefaciens* C58. The *aaeR-aaeXAB* and *slyA-ydhIJK* gene clusters were found to be present in *Pantoea ananatis* LMG20103, *Pantoea agglomerans* C410P1, *Enterobacter cloacae* subsp. *cloacae* ATCC13047, *Enterobacter cancerogenus* CR-Eb1, *Shigella flexneri* 301, *Salmonellaenterica* subsp. *enterica serovar Typhimurium* LT2, and *Escherichia coli* K12 (Figure 8). Interestingly, the *slyA* gene was present, but the *ydhIJK* efflux pump coding genes were absent in several strains, including *Pectobacterium carotovorum* subsp. *carotovorum* PC1,

https://doi.org/10.1021/acs.jafc.5c03670
J. Agric. Food Chem. 2025, 73, 17458−17470

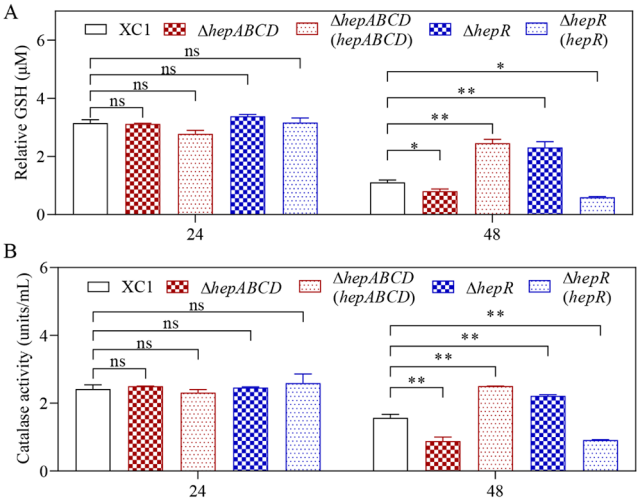

Figure 4. HepABCD efflux pump modulates the levels of catalase and GSH in Xcc. (A) GSH levels of XC1, Δ*hepABCD*, Δ*hepABCD* (*hepABCD*), Δ*hepR*, and Δ*hepR* (*hepR*) at 24 and 48 hpi. (B) Catalase activity levels of XC1, Δ*hepABCD*, Δ*hepABCD* (*hepABCD*), Δ*hepR*, and Δ*hepR* (*hepR*) at 24 and 48 hpi. Shown are the averages of three technical repeats with the standard deviation. Statistically significant differences are indicated by one asterisk ($p < 0.01$) or two asterisks ($p < 0.01$).

Pectobacterium actinidiae GX-Pa1, *Dickeya zeae* EC1, *Dickeya dadantii* 3937, *Erwinia amylovora* ATCC 49946, and *Erwinia pyrifoliae* DSM 12163 (Figure 8). These findings suggested that the *aaeR-aaeXAB* and *slyA-ydhIJK* systems are usually both present in bacterial strains. However, *hepR-hepABCD* appeared to function independently and was not observed to coexist with either *aaeR-aaeXAB* or *slyA-ydhIJK* in any strain.

DISCUSSION

In response to microbial invasion, one defense mechanism employed by plants is to synthesize and accumulate phenolic compounds.[19] Previous studies showed that Xcc can degrade certain phenolic compounds to safeguard infection.[7,11] However, some plant phenolic compounds are resistant to Xcc degradation.[11] In this study, we demonstrated that the Xcc RND family efflux pump HepABCD is key to expelling benzoic acid, cinnamic acid, and many of their monohydroxylated derivatives (Table 1, Figure 2). This mechanism enables Xcc to cope with the release of this group of phenolic compounds by the host plant. Additionally, HepABCD helps manage ROS stress in Xcc by regulating catalase and GSH production (Figure 4). Regarding the regulatory mechanisms, we found that the transcriptional regulator HepR can sense 4-HBA and the redox state to regulate the expression of *hepABCD* (Figures 5 and 7). The *hepR-hepABCD* system is widely distributed among various plant pathogens (Figure 8), suggesting that this system is a conserved pathogenic component. Collectively, our findings revealed the molecular mechanisms by which pathogens cope with antimicrobial phenolic compounds within plants.

As a vascular pathogen, Xcc is exposed to large amounts of phenolic acids produced by plants during infection. RND family efflux pumps are transmembrane transporters widely distributed among plant pathogens, and they export a broad range of toxic compounds, including lipophilic, cationic, neutral (chloramphenicol and solvents), and acidic (β-lactams) compounds.[33−35] In Gram-negative bacteria, RND efflux systems exhibit distinct yet complementary substrate preferences and can effectively extrude most clinically relevant antibiotics from the bacterial cell.[36] However, only a limited number of RND family efflux systems associated with multidrug resistance in phytopathogens have been characterized. The RND transporter IfeAB in *Agrobacterium tumefaciens* exports isoflavonoids, which are antimicrobial plant metabolites.[37] Similarly, the AcrAB efflux system in *Erwinia amylovora* is crucial for resistance against antimicrobial plant metabolites and for the successful colonization of host plants.[38] The AaeAB efflux system has a narrow substrate specificity limited to hydroxylated aromatic carboxylic acids, including 4-HBA, 6-hydroxy-2-naphthoic acid, and 2-hydroxycinnamate.[21] Although HepB in Xcc shares 40.55% amino acid identity with AaeA in *E. coli* (Fig. S1), our study revealed distinct substrate specificities between HepABCD and AaeXAB. HepABCD effectively expelled benzoic acid, cinnamic acid, and their derivatives containing a single hydroxyl group, but not benzoic or cinnamic acid compounds with multiple hydroxyl groups (Figures 2 and S1). Intriguingly, *hepR-hepABCD* appeared to function independently and was not observed to coexist with either *aaeR-aaeXAB* or *slyA-ydhIJK* in any strain (Figure 8). This finding suggested that, over the course of natural selection, different plant pathogens developed distinct efflux pumps to expel antibacterial compounds, enabling them to adapt to the diverse types of phenolic compounds encountered in various host plants.

RND efflux pump expression in bacterial pathogens is often induced by various molecules, including bile, biocides, pharmaceuticals, additives, and plant extracts.[39] HepR was previously reported as a sensor for SA in Xcc and is conserved across a range of bacterial plant pathogens.[17] Our current results demonstrated that SA, 4-HBA, and their analogs induce *hep* gene cluster expression in a cumulative manner (Figure S4). Furthermore, our latest findings combined with current data suggested that HepR exhibits a broad substrate-binding capability, allowing it to sense SA, CA, 2-HCA, and 4-HBA.[40] We are actively investigating the crystal structures of HepR in complex with these compounds, aiming to provide insights into the structural basis of the broad substrate specificity of HepR.

In addition to the ability of bacterial RND efflux pumps to expel a broad spectrum of bioactive molecules, their expression is also regulated by various systems[35] that respond to multiple environmental signals, including pH, the presence of antimicrobials, divalent metal ions, organic solvents, the growth phase, and oxidative stress.[41,42] Oxidative stress is typically characterized by ROS production in host cells, which represents a strategy to limit the spread of pathogens during the early stages of host−pathogen interactions.[43] Pathogens must therefore mitigate the harmful effects of host-generated ROS to prevent their invasion. Our study demonstrated that the HepABCD efflux pump is involved in the antioxidant defense of Xcc, modulating the biosynthesis of key antioxidative molecules, including GSH and catalase (Figures 3 and 4). Further investigation revealed that two cysteine residues in HepR, C39 and C77, are essential for sensing the redox state that regulates *hepABCD* gene expression (Figure 7). This mechanism likely allows Xcc to eliminate phenolic compounds during infection while simultaneously managing the excessive ROS generated by the plant immune response. This complex regulatory network indicates that the promiscuous transport activities of major primordial pumps may have been exploited for diverse cellular functions.[44] However, to fully elucidate the mode of action of HepABCD, the signaling pathways linking HepABCD to antioxidant activity in Xcc require further investigation.

https://doi.org/10.1021/acs.jafc.5c03670
J. Agric. Food Chem. 2025, 73, 17458−17470

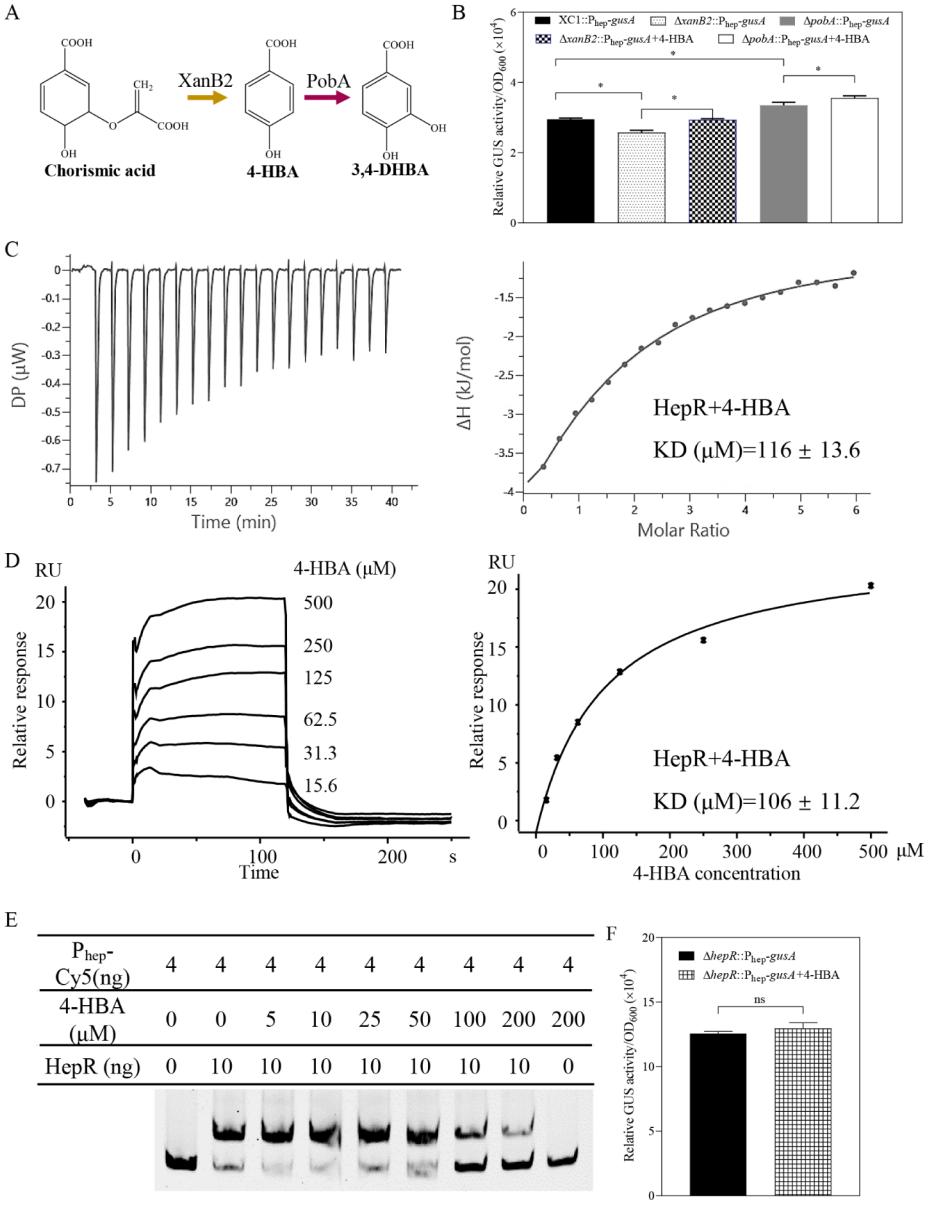

Figure 5. Transcription of the *hepR-hepABCD* gene cluster is induced by 4-HBA. (A) *Xcc* synthesized 4-HBA via chorismatase XanB2 and degraded 4-HBA via 3-hydroxylase PobA. (B) The relative GUS activity of the reporter strains of XC1:P_{hep}-*gusA*, Δ*pobA*::P_{hep}-*gusA*, and Δ*xanB2*::P_{hep}-*gusA*, with or without 100 μM 4-HBA 12 hpi. (C) Isothermal titration calorimetry (ITC) analysis of the binding between 4-HBA and HepR. (D) Surface plasmon resonance (SPR) analysis of the interaction between 4-HBA and HepR. (E) EMSA assay showed that high levels of 4-HBA prevented HepR from binding to the promoter P_{hep}. (F) The relative GUS activity of the reporter strain Δ*hepR*::P_{hep}-*gusA* with or without 100 μM 4-HBA 12 hpi.

Previously, 4-HBA was associated with biofilm formation modulation, EPS production, and pathogenicity in *Shigella sonnei*,[20] as well as the production of the antifungal metabolite heat-stable antifungal factor (HSAF), which provides a competitive advantage to *Lysobacter enzymogenes*.[45] In this study, we found that HepR can regulate both intracellular and extracellular 4-HBA levels via HepABCD (Figure 1C,D). Our previous study demonstrated that 4-HBA is a precursor of coenzyme Q (CoQ) and xanthomonadin synthesis in Xcc, both of which have crucial roles in antioxidant activity.[46,47] However, deleting *hepR* or *hepABCD* had no significant effect on xanthomonadin or CoQ levels (Figure S5). Further investigations are needed to fully elucidate the biological functions affected by 4-HBA in Xcc.

4-HBA was previously demonstrated to modulate the regulatory activity of several transcriptional regulators, including $LysR_{Le}$ and AaeR,[20,45] which in turn, regulate the virulence of certain phytopathogens.[7,12] This study identified HepR as an additional 4-HBA sensor, albeit with weak binding affinity (K_d ~ 100 μM) (Figure 5C,D). PobR, which regulates 4-HBA degradation in Xcc, also serves as a 4-HBA sensor but with a significantly stronger binding affinity (K_d = 4.3 μM).[7] This suggests that HepR may be more suited to sense exogenous 4-HBA or that other phenolic compounds produced by plants are more likely to trigger 4-HBA efflux. Therefore, we hypothesize that Xcc prioritizes the 4-HBA degradation pathway when 4-HBA levels are low, but under survival stresses caused by high levels of 4-HBA or other phenolic compounds, it uses the HepABCD efflux system to expel excess compounds. The

https://doi.org/10.1021/acs.jafc.5c03670
J. Agric. Food Chem. 2025, 73, 17458−17470

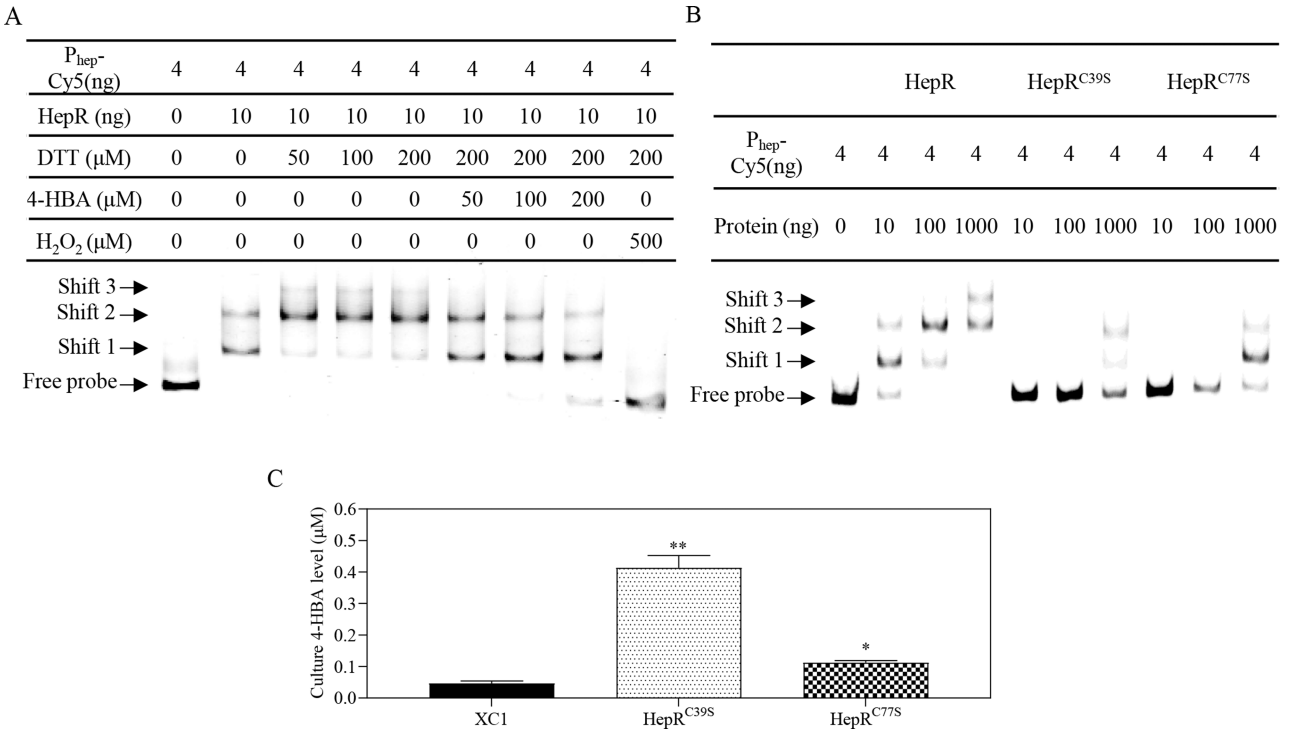

Figure 6. HepR is a redox sensor. (A) EMSA analysis of the P_{hep} binding capacity of HepR in the presence of DTT and 4-HBA. (B) EMSA analysis of the P_{hep} binding capacity of HepR, $HepR^{C39S}$, and $HepR^{C77S}$ mutant proteins. (C) Extracellular 4-HBA levels of the Xcc strains XC1, $HepR^{C39S}$, and $HepR^{C77S}$ in XYS medium 12 hpi. Shown are the averages of three technical repeats with the standard deviation. Statistically significant differences are indicated by one asterisk ($p < 0.05$) or two asterisks ($p < 0.01$).

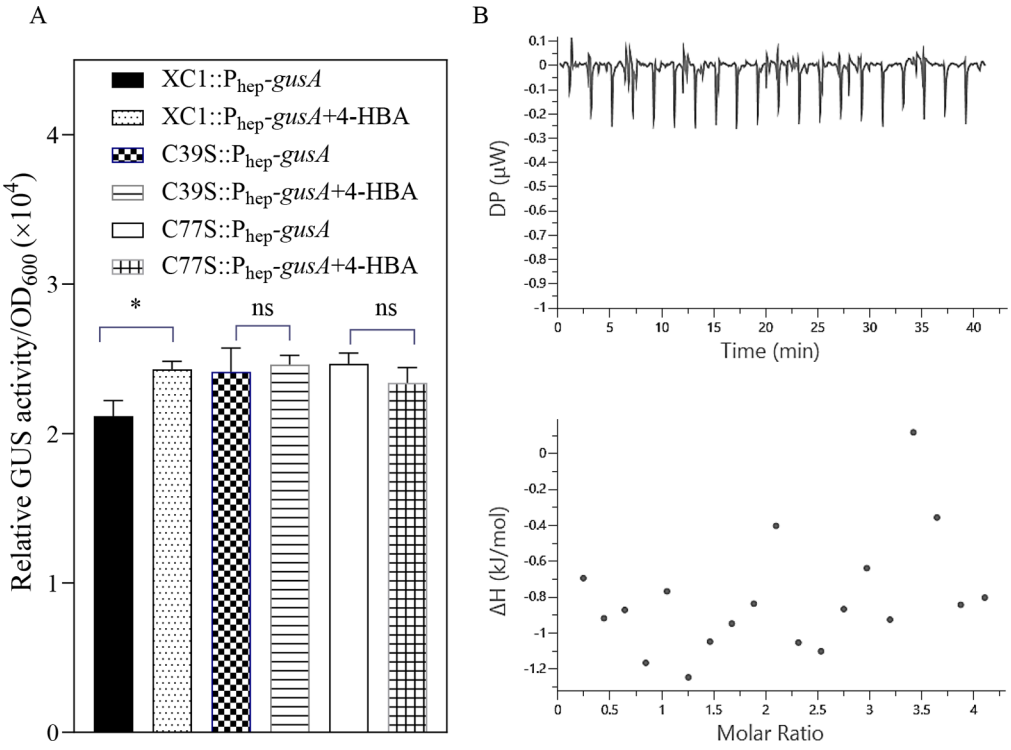

Figure 7. $C^{39}$and $C^{77}$are essential for HepR binding to 4-HBA. (A) The relative GUS activity of the reporter strains of XC1:P_{hep}-*gusA*, C39S:P_{hep}-*gusA*, and C77S:P_{hep}-*gusA*, with or without 100 μM 4-HBA 12 hpi. (B) ITC analysis of the binding between 4-HBA and the $HepR^{C39S}$ mutant. Shown are the averages of three technical repeats with the standard deviation. Statistically significant differences are indicated by one asterisk ($p < 0.05$).

mechanisms by which Xcc coordinates the degradation and efflux of 4-HBA through two transcription factors (HepR and PobR) and the potential cross-regulation of signaling pathways are currently under investigation.

https://doi.org/10.1021/acs.jafc.5c03670
J. Agric. Food Chem. 2025, 73, 17458−17470

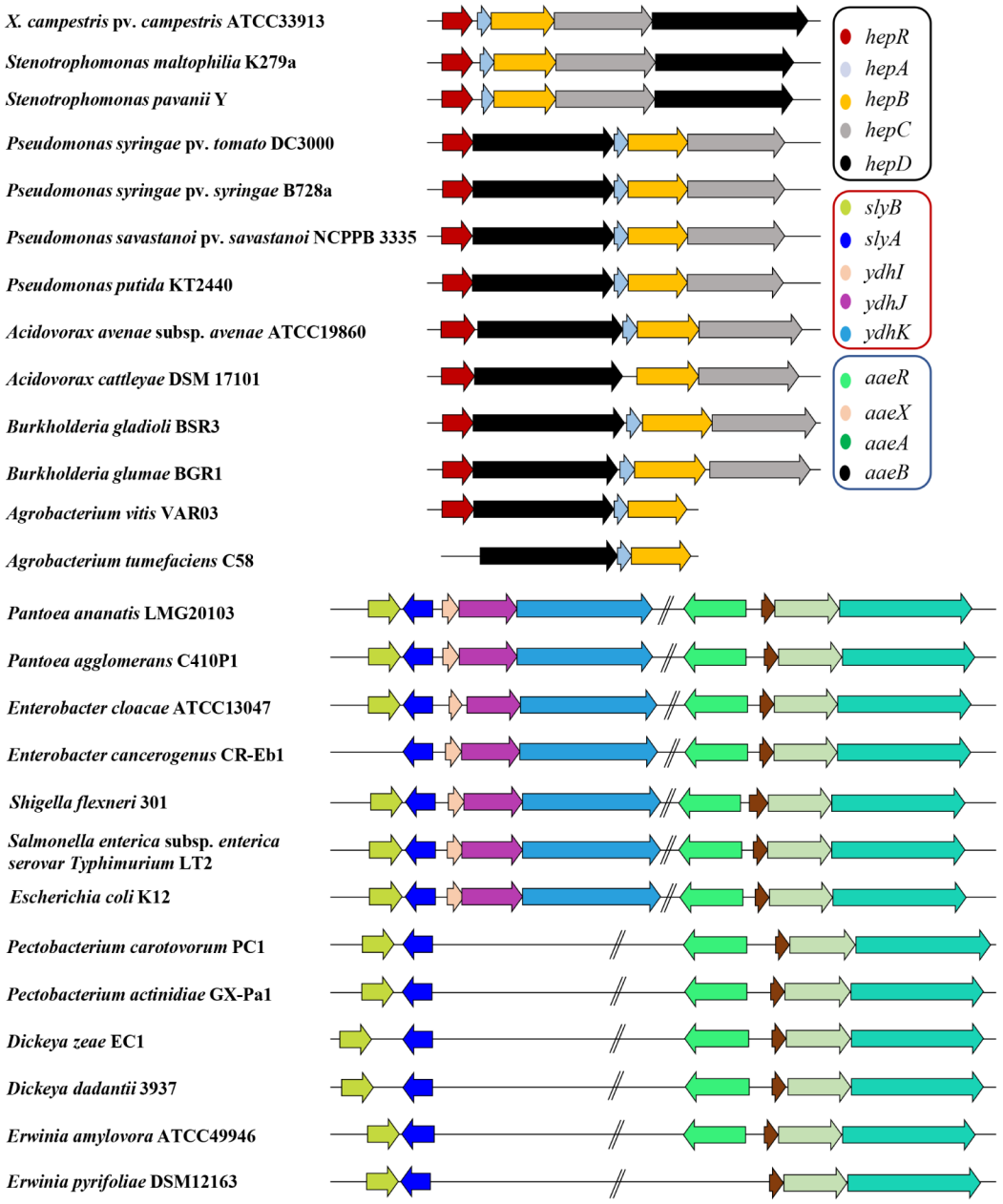

Figure 8. Distribution of *hepR-hepABCD*, *slyA-ydhIJK*, and *aaeR-aaeXAB* across various bacteria species.

■ ASSOCIATED CONTENT

Data Availability Statement

The authors confirm that all data supporting the findings of this study are contained within the article and its Supporting Information.

Supporting Information

The Supporting Information is available free of charge at https://pubs.acs.org/doi/10.1021/acs.jafc.5c03670.

Information of bacterial strains used in this study (Table S1); plasmids used in this study (Table S2); oligonucleotide primers used in this study (Table S3); comparison of the *hepABCD* gene cluster with the *aaeXAB* gene cluster (Figure S1); tolerance of benzoic and cinnamic analogs on growth of XC1 strains with and without the HepABCD efflux pump (Figure S2); W22 is a crucial amino acid residue for HepR binding to both SA and 4-HBA. (Figure S3); SA and 4-HBA analogues have cumulative effects on inducing hep gene cluster expression (Figure S4); the effect of HepR and HepABCD on Coenzyme Q and xanthomonadin level (Figure S5) (PDF)

■ AUTHOR INFORMATION

Corresponding Authors

Lian Zhou − *Zhiyuan Innovative Research Center, Student Innovation Center, Zhiyuan College, Shanghai Jiao Tong University, Shanghai 200240, China;* orcid.org/0000-0001-8752-2562; Email: lianzhou@sjtu.edu.cn

Ya-Wen He − *State Key Laboratory of Microbial Metabolism, Joint International Research Laboratory of Metabolic and Developmental Sciences, School of Life Sciences and Biotechnology, Shanghai Jiao Tong University, Shanghai 200240, China;* orcid.org/0000-0002-7349-924X; Email: yawenhe@sjtu.edu.cn

Authors

Kai Song − *State Key Laboratory of Microbial Metabolism, Joint International Research Laboratory of Metabolic and Developmental Sciences, School of Life Sciences and Biotechnology, Shanghai Jiao Tong University, Shanghai 200240, China;* orcid.org/0009-0003-4624-158X

Ying Cui − *State Key Laboratory of Microbial Metabolism, Joint International Research Laboratory of Metabolic and Developmental Sciences, School of Life Sciences and Biotechnology, Shanghai Jiao Tong University, Shanghai 200240, China*

Lin Li − *State Key Laboratory of Microbial Metabolism, Joint International Research Laboratory of Metabolic and Developmental Sciences, School of Life Sciences and Biotechnology, Shanghai Jiao Tong University, Shanghai 200240, China*

Jia-Yuan Wang − *State Key Laboratory of Microbial Metabolism, Joint International Research Laboratory of Metabolic and Developmental Sciences, School of Life Sciences and Biotechnology, Shanghai Jiao Tong University, Shanghai 200240, China*

Si-Nan Li − *State Key Laboratory of Microbial Metabolism, Joint International Research Laboratory of Metabolic and Developmental Sciences, School of Life Sciences and Biotechnology, Shanghai Jiao Tong University, Shanghai 200240, China*

Yu-Cheng Gu − *Jealott's Hill International Research Center, Syngenta, Berkshire RE42 6EY, U.K.;* orcid.org/0000-0002-6400-6167

Complete contact information is available at: https://pubs.acs.org/10.1021/acs.jafc.5c03670

Author Contributions

K.S.: investigation and methodology. Y.C., J.-Y.W., and L.L.: data analysis. Y.-C.G. and S.-N.L.: methodology. L.Z., Y.-W.H.: supervision and funding acquisition. K.S., L.Z., and Y.-W.H.: conceptualization, writing—review and editing. All authors read and approved the manuscript.

Funding

This work was financially supported by research grants from the National Natural Science Foundation of China (nos. 31972231 and 32172355 to HYW) and the Startup Fund for Young Faculty at SJTU (SFYF at SJTU to K.S.).

Notes

The authors declare no competing financial interest.

REFERENCES

(1) Vicente, J. G.; Holub, E. B. *Xanthomonas campestris* pv. *campestris* (cause of black rot of crucifers) in the genomic era is still a worldwide threat to brassica crops. *Mol. Plant Pathol.* **2013**, *14*, 2−18.

(2) Timilsina, S.; Potnis, N.; Newberry, E. A.; Liyanapathiranage, P.; Iruegas-Bocardo, F.; White, F. F.; Goss, E. M.; Jones, J. B. *Xanthomonas* diversity, virulence and plant-pathogen interactions. *Nat. Rev. Microbiol.* **2020**, *18*, 415−427.

(3) Qian, W.; Jia, Y.; Ren, S. X.; He, Y. Q.; Feng, J. X.; Lu, L. F.; Sun, Q.; Ying, G.; Tang, D. J.; Tang, H.; Wu, W.; Hao, P.; Wang, L.; Jiang, B. L.; Zeng, S.; Gu, W. Y.; Lu, G.; Rong, L.; Tian, Y.; Yao, Z.; Fu, G.; Chen, B.; Fang, R.; Qiang, B.; Chen, Z.; Zhao, G. P.; Tang, J. L.; He, C. Comparative and functional genomic analyses of the pathogenicity of phytopathogen *Xanthomonas campestris* pv. *Campestris*. *Genome Res.* **2005**, *15*, 757−767.

(4) Bhattacharya, A.; Sood, P.; Citovsky, V. The roles of plant phenolics in defence and communication during *Agrobacterium* and *Rhizobium* infection. *Mol. Plant Pathol.* **2010**, *11*, 705−719.

(5) Fitzgerald, D. J.; Stratford, M.; Gasson, M. J.; Ueckert, J.; Bos, A.; Narbad, A. Mode of antimicrobial action of vanillin against *Escherichia coli*, *Lactobacillus plantarum* and *Listeria innocua*. *J. Appl. Microbiol.* **2004**, *97*, 104−113.

(6) Harris, V.; Jiranek, V.; Ford, C. M.; Grbin, P. R. Inhibitory effect of hydroxycinnamic acids on *Dekkera* spp. *Appl. Microbiol. Biotechnol.* **2010**, *86*, 721−729.

(7) Chen, B.; Li, R. F.; Zhou, L.; Qiu, J. H.; Song, K.; Tang, J. L.; He, Y. W. The phytopathogen *Xanthomonas campestris* utilizes the divergently transcribed *pobA*/*pobR* locus for 4-hydroxybenzoic acid recognition and degradation to promote virulence. *Mol. Microbiol.* **2020**, *114*, 870−886.

(8) Sircar, D.; Mitra, A. Evidence for *p*-hydroxybenzoate formation involving enzymatic phenylpropanoid side-chain cleavage in hairy roots of Daucus carota. *J. Plant Physiol.* **2008**, *165*, 407−414.

(9) Lowe, T. M.; Ailloud, F.; Allen, C. Hydroxycinnamic Acid Degradation, a Broadly Conserved Trait, Protects *Ralstonia solanacearum* from Chemical Plant Defenses and Contributes to Root Colonization and Virulence. *Mol. Plant Microbe. Interact* **2015**, *28*, 286−297.

(10) Cogan, D. P.; Baraquet, C.; Harwood, C. S.; Nair, S. K. Structural basis of transcriptional regulation by CouR, a repressor of coumarate catabolism, in *Rhodopseudomonas palustris*. *J. Biol. Chem.* **2018**, *293*, 11727−11735.

(11) Chen, B.; Li, R. F.; Zhou, L.; Song, K.; Poplawsky, A. R.; He, Y.-W. The phytopathogen *Xanthomonas campestris* scavenges hydroxycinnamic acids *in planta* via the *hca* cluster to increase virulence on its host plant. *Phytopathol. Res.* **2022**, *4* (1), 12.

(12) Wang, J.-Y.; Zhou, L.; Chen, B.; Sun, S.; Zhang, W.; Li, M.; Tang, H.; Jiang, B.-L.; Tang, J.-L.; He, Y.-W. A functional 4-hydroxybenzoate degradation pathway in the phytopathogen *Xanthomonas campestris* is required for full pathogenicity. *Sci. Rep.* **2015**, *5*, 18456.

(13) Thekkiniath, J.; Ravirala, R.; San Francisco, M. Multidrug Efflux Pumps in the Genus Erwinia: Physiology and Regulation of Efflux Pump Gene Expression. *Prog. Mol. Biol. Transl. Sci.* **2016**, *142*, 131−149.

(14) Pasqua, M.; Grossi, M.; Zennaro, A.; Fanelli, G.; Micheli, G.; Barras, F.; Colonna, B.; Prosseda, G. The Varied Role of Efflux Pumps of the MFS Family in the Interplay of Bacteria with Animal and Plant Cells. *Microorganisms* **2019**, *7*, 285.

(15) Ravirala, R. S.; Barabote, R. D.; Wheeler, D. M.; Reverchon, S.; Tatum, O.; Malouf, J.; Liu, H.; Pritchard, L.; Hedley, P. E.; Birch, P. R.; Toth, I. K.; Payton, P.; San Francisco, M. J. Efflux pump gene expression in *Erwinia chrysanthemi* is induced by exposure to phenolic acids. *Mol. Plant Microbe. Interact* **2007**, *20*, 313−320.

(16) Barabote, R. D.; Johnson, O. L.; Zetina, E.; San Francisco, S. K.; Fralick, J. A.; San Francisco, M. J. *Erwinia chrysanthemi tolC* is involved in resistance to antimicrobial plant chemicals and is essential for phytopathogenesis. *J. Bacteriol.* **2003**, *185*, 5772−5778.

(17) Song, K.; Li, R.; Cui, Y.; Chen, B.; Zhou, L.; Han, W.; Jiang, B.-L.; He, Y.-W. The phytopathogen *Xanthomonas campestris* senses and effluxes salicylic acid via a sensor HepR and an RND family efflux pump to promote virulence in host plants. *mLife* **2024**, *3*, 430−444.

(18) Zhou, L.; Wang, J.-Y.; Wang, J.; Poplawsky, A.; Lin, S.; Zhu, B.; Chang, C.; Zhou, T.; Zhang, L.-H.; He, Y.-W. The diffusible factor synthase XanB2 is a bifunctional chorismatase that links the shikimate pathway to ubiquinone and xanthomonadins biosynthetic pathways. *Mol. Microbiol.* **2013**, *87* (1), 80−93.

(19) Báidez, A. G.; Gómez, P.; Del Río, J. A.; Ortuño, A. Dysfunctionality of the xylem in Olea europaea L. Plants associated with the infection process by Verticillium dahliae Kleb. Role of phenolic compounds in plant defense mechanism. *J. Agric. Food Chem.* **2007**, *55*, 3373−3377.

(20) Wang, M.; Zeng, J.; Zhu, Y.; Chen, X.; Guo, Q.; Tan, H.; Cui, B.; Song, S.; Deng, Y. A 4-Hydroxybenzoic Acid-Mediated Signaling System Controls the Physiology and Virulence of *Shigella sonnei*. *Microbiol. Spectrum.* **2023**, *11* (3), No. e0483522.

(21) Van Dyk, T. K.; Templeton, L. J.; Cantera, K. A.; Sharpe, P. L.; Sariaslani, F. S. Characterization of the *Escherichia coli* AaeAB efflux pump: a metabolic relief valve? *J. Bacteriol.* **2004**, *186*, 7196−7204.
(22) Borisov, V. B.; Siletsky, S. A.; Nastasi, M. R.; Forte, E. ROS Defense Systems and Terminal Oxidases in Bacteria. *Antioxidants* **2021**, *10*, 839.
(23) Schmacht, M.; Lorenz, E.; Senz, M. Microbial production of glutathione. *World J. Microbiol. Biotechnol.* **2017**, *33*, 106.
(24) Yuan, F.; Yin, S.; Xu, Y.; Xiang, L.; Wang, H.; Li, Z.; Fan, K.; Pan, G. The Richness and Diversity of Catalases in Bacteria. *Front. Microbiol.* **2021**, *12*, 645477.
(25) Gebicka, L.; Krych-Madej, J. The role of catalases in the prevention/promotion of oxidative stress. *J. Inorg. Biochem.* **2019**, *197*, 110699.
(26) Gullner, G.; Tóbiás, I.; Fodor, J.; Kömives, T. Elevation of glutathione level and activation of glutathione-related enzymes affect virus infection in tobacco. *Free Radic Res.* **1999**, *31*, 155−161.
(27) Hernández, L. E.; Sobrino-Plata, J.; Montero-Palmero, M. B.; Carrasco-Gil, S.; Flores-Cáceres, M. L.; Ortega-Villasante, C.; Escobar, C. Contribution of glutathione to the control of cellular redox homeostasis under toxic metal and metalloid stress. *J. Exp. Bot.* **2015**, *66*, 2901−2911.
(28) Panmanee, W.; Vattanaviboon, P.; Eiamphungporn, W.; Whangsuk, W.; Sallabhan, R.; Mongkolsuk, S. OhrR, a transcription repressor that senses and responds to changes in organic peroxide levels in *Xanthomonas campestris* pv. *Phaseoli. Mol. Microbiol.* **2002**, *45*, 1647−1654.
(29) Lee, S. J.; Lee, I.-G.; Lee, K. Y.; Kim, D.-G.; Eun, H.-J.; Yoon, H.-J.; Chae, S.; Song, S.-H.; Kang, S.-O.; Seo, M.-D.; et al. Two distinct mechanisms of transcriptional regulation by the redox sensor YodB. *Proc. Natl. Acad. Sci. U. S. A.* **2016**, *113* (35), No. E5202−E5211.
(30) Si, M.; Chen, C.; Che, C.; Liu, Y.; Li, X.; Su, T. The thiol oxidation-based sensing and regulation mechanism for the OasR-mediated organic peroxide and antibiotic resistance in *C. glutamicum*. *Biochem. J.* **2020**, *477*, 3709−3727.
(31) Fassler, R.; Zuily, L.; Lahrach, N.; Ilbert, M.; Reichmann, D. The Central Role of Redox-Regulated Switch Proteins in Bacteria. *Front. Mol. Biosci.* **2021**, *8*, 706039.
(32) Will, W. R.; Brzovic, P.; Le Trong, I.; Stenkamp, R. E.; Lawrenz, M. B.; Karlinsey, J. E.; Navarre, W. W.; Main-Hester, K.; Miller, V. L.; et al. The Evolution of SlyA/RovA Transcription Factors from Repressors to Countersilencers in *Enterobacteriaceae*. *mBio* **2019**, *10* (2), No. e00009−19.
(33) Nikaido, H.; Pagès, J. M. Broad-specificity efflux pumps and their role in multidrug resistance of Gram-negative bacteria. *FEMS Microbiol. Rev.* **2012**, *36*, 340−363.
(34) Du, D.; Wang-Kan, X.; Neuberger, A.; van Veen, H. W.; Pos, K. M.; Piddock, L. J. V.; Luisi, B. F. Multidrug efflux pumps: structure, function and regulation. *Nat. Rev. Microbiol.* **2018**, *16*, 523−539.
(35) Henderson, P. J. F.; Maher, C.; Elbourne, L. D. H.; Eijkelkamp, B. A.; Paulsen, I. T.; Hassan, K. A. Physiological Functions of Bacterial "Multidrug" Efflux Pumps. *Chem. Rev.* **2021**, *121*, 5417−5478.
(36) Zgurskaya, H. I.; Malloci, G.; Chandar, B.; Vargiu, A. V.; Ruggerone, P. Bacterial efflux transporters' polyspecificity - a gift and a curse? *Curr. Opin. Microbiol.* **2021**, *61*, 115−123.
(37) Palumbo, J. D.; Kado, C. I.; Phillips, D. A. An isoflavonoid-inducible efflux pump in *Agrobacterium tumefaciens* is involved in competitive colonization of roots. *J. Bacteriol.* **1998**, *180*, 3107−3113.
(38) Burse, A.; Weingart, H.; Ullrich, M. S. The phytoalexin-inducible multidrug efflux pump AcrAB contributes to virulence in the fire blight pathogen, *Erwinia amylovora*. *Mol. Plant Microbe. Interact* **2004**, *17*, 43−54.
(39) Novelli, M.; Bolla, J. M. RND Efflux Pump Induction: A Crucial Network Unveiling Adaptive Antibiotic Resistance Mechanisms of Gram-Negative Bacteria. *Antibiotics* **2024**, *13*, 501.
(40) Song, K.; Cui, Y.; Li, S. N.; Li, L.; Zhou, L.; Tian, D. L.; Gu, Y. C.; He, Y. W. Hydroxycinnamic Acids Activate RpfB-Dependent Quorum Sensing Signal Turnover in Phytopathogen *Xanthomonas campestris*. *J. Agric. Food Chem.* **2025**, *73*, 3990−4000.
(41) Ruiz, C.; Levy, S. B. Regulation of *acrAB* expression by cellular metabolites in *Escherichia coli*. *J. Antimicrob. Chemother.* **2014**, *69*, 390−399.
(42) Keseler, I. M.; Mackie, A.; Santos-Zavaleta, A.; Billington, R.; Bonavides-Martínez, C.; Caspi, R.; Fulcher, C.; Gama-Castro, S.; Kothari, A.; Krummenacker, M.; et al. The EcoCyc database: reflecting new knowledge about *Escherichia coli* K-12. *Nucleic Acids Res.* **2017**, *45*, D543−D550.
(43) Zhang, J.; Li, H.; Gu, W.; Zhang, K.; Liu, X.; Liu, M.; Yang, L.; Li, G.; Zhang, Z.; Zhang, H. Peroxisome dynamics determines host-derived ROS accumulation and infectious growth of the rice blast fungus. *mBio* **2023**, *14* (6), No. e0238123.
(44) Kumawat, M.; Nabi, B.; Daswani, M.; Viquar, I.; Pal, N.; Sharma, P.; Tiwari, S.; Sarma, D. K.; Shubham, S.; Kumar, M. Role of bacterial efflux pump proteins in antibiotic resistance across microbial species. *Microb. Pathog.* **2023**, *181*, 106182.
(45) Su, Z.; Chen, H.; Wang, P.; Tombosa, S.; Du, L.; Han, Y.; Shen, Y.; Qian, G.; Liu, F. 4-Hydroxybenzoic acid is a diffusible factor that connects metabolic shikimate pathway to the biosynthesis of a unique antifungal metabolite in *Lysobacter enzymogenes*. *Mol. Microbiol.* **2017**, *104*, 163−178.
(46) Cao, X.-Q.; Wang, J.-Y.; Zhou, L.; Chen, B.; Jin, Y.; He, Y.-W. Biosynthesis of the yellow xanthomonadin pigments involves an ATP-dependent 3-hydroxybenzoic acid: acyl carrier protein ligase and an unusual type II polyketide synthase pathway. *Mol. Microbiol.* **2018**, *110* (1), 16−32.
(47) Cao, X. Q.; Ouyang, X. Y.; Chen, B.; Song, K.; Zhou, L.; Jiang, B. L.; Tang, J. L.; Ji, G.; Poplawsky, A. R.; He, Y. W. Genetic Interference Analysis Reveals that Both 3-Hydroxybenzoic Acid and 4-Hydroxybenzoic Acid Are Involved in Xanthomonadin Biosynthesis in the Phytopathogen *Xanthomonas campestris* pv. *Campestris*. *Phytopathol.* **2020**, *110*, 278−286.

https://doi.org/10.1021/acs.jafc.5c03670
J. Agric. Food Chem. 2025, 73, 17458−17470